HHS Public Access

Author manuscript

Nat Med. Author manuscript; available in PMC 2011 July 13.

Published in final edited form as:

Nat Med. 2011 January ; 17(1): 55–63. doi:10.1038/nm.2277.

The Pleiotropic Actions of Adiponectin are Initiated via Receptor-Mediated Activation of Ceramidase Activity

William L. Holland[1], **Russell A. Miller**[2], **Zhao V. Wang**[1], **Kai Sun**[1], **Brian M. Barth**[3], **Hai H. Bui**[4], **Kathryn E. Davis**[1], **Benjamin T. Bikman**[5], **Nils Halberg**[1,6], **Joseph M. Rutkowski**[1], **Mark R. Wade**[4], **Vincent M. Tenorio**[1], **Ming-Shang Kuo**[4], **Joseph T. Brozinick**[4], **Bei B. Zhang**[7], **Morris J. Birnbaum**[2], **Scott A. Summers**[3,5], and **Philipp E. Scherer**[1,8,*]

[1]Touchstone Diabetes Center, Department of Internal Medicine, The University of Texas Southwestern Medical Center, Dallas, Texas 75390-8549

[2]Department of Medicine, Institute for Diabetes, Obesity and Metabolism, University of Pennsylvania School of Medicine, Philadelphia, PA 19104

[3]Department of Biochemistry and Molecular Biology, Colorado State University, Fort Collins, CO 80523

[4]Eli Lilly and Company, Lilly Corporate Center, Indianapolis, IN 46285

[5]Program in Cardiovascular and Metabolic Diseases, Duke-NUS Graduate Medical School, Singapore, 169857 and the Stedman Center for Nutrition and Metabolism Research, Duke University Medical Center, Durham, NC 277044

[6]Department of Biomedical Sciences, Faculty of Health Science, University of Copenhagen, Copenhagen 2100, Denmark

[7]Department of Metabolic Disorders, Merck Research Laboratories, Rahway, NJ 07065

[8]Department of Cell Biology, The University of Texas Southwestern Medical Center, Dallas, Texas 75390-8549

Abstract

The adipocyte-derived secretory factor adiponectin promotes insulin sensitivity, decreases inflammation and promotes cell survival. To date, no unifying mechanism explains how

*corresponding author: philipp.scherer@utsouthwestern.eduTelephone: (214) 648-8715 Fax: (214) 648-8720.

Author Contributions W.L.H. conducted all experiment except the portions indicated below and contributed to the writing of the manuscript.

R.A.M. conducted in vivo experiments with liver-specific LKB1$^{-/-}$ mice.

Z.V.W. generated all of the ATTAC mouse models used here.

K.S was responsible for the mutagenesis studies of adipoR1 and adipoR2.

B.M.B. was involved in the studies with INS-1 cells.

H.H.B.; M.R.W.; M.S.K.; J.T.B. were involved in LC-MS/MS analysis for determination of sphingolipid content of the samples.

K.E.D assisted in the generation of the adipoR1/2$^{-/-}$ MEFs and high fat feeding studies using adiponectin transgenic mice.

B.T.B. helped in data analysis and rtPCR of sphingolipid metabolism genes.

N.H. performed the experiments with *in vivo* injections of adiponectin and detection of the protein in β cells.

J.M.R. was involved in designing experiments and protein production.

V.M.T. performed ceramidase assays and genotyping.

B.B.Z.; M.J.B; S.A.S; P.E.S. were involved in experimental design, data analysis and in the writing of the manuscript.

adiponectin can exert such a variety of beneficial systemic effects. Here, we show that adiponectin potently stimulates a ceramidase activity associated with its two receptors, adipoR1 and adipoR2, and enhances ceramide catabolism and formation of its anti-apoptotic metabolite – sphingosine-1-phosphate (S1P), independently of AMPK. Using models of inducible apoptosis in pancreatic β-cells and cardiomyocytes, we show that transgenic overproduction of adiponectin decreases caspase-8 mediated death, while genetic adiponectin ablation enhances apoptosis *in vivo* through a sphingolipid-mediated pathway. Ceramidase activity is impaired in cells lacking both adiponectin receptor isoforms, leading to elevated ceramide levels and enhanced susceptibility to palmitate-induced cell death. Combined, our observations suggest a novel unifying mechanism of action for the beneficial systemic effects exerted by adiponectin, with sphingolipid metabolism as its core upstream component.

Introduction

Adiponectin is emerging as a protein with insulin-sensitizing, anti-inflammatory and anti-apoptotic functions. However, the underlying mechanistic basis for its pleiotropic actions is missing. Adiponectin is released by adipocytes and targets a multitude of different cell types. Prominent target cells are hepatocytes, cardiac myocytes, pancreatic β cells and podocytes. Two related receptors have been cloned, AdipoR1 and AdipoR2, which may mediate some of the actions of adiponectin[1]. Overexpression of adiponectin from adipose tissue results in improvements in systemic insulin sensitivity[2–3], whereas loss of function of adiponectin or its receptors results in decreased insulin sensitivity.

Sphingolipids, such as ceramide and glucosylceramides, are an important class of bioactive lipids. Aberrant accumulation of ceramide, glucosylceramide, and GM3 ganglioside has been implicated in a multitude of metabolic processes including atherosclerosis, insulin resistance and lipotoxic heart failure (reviewed in[4]). In contrast, the phosphorylated sphingoid base Sphingosine 1-phosphate (S1P) is a potent inducer of proliferation and inhibitor of apoptosis[5]. The opposing nature and simple 2-step conversion process separating these lipids has led to speculation that the dynamic ratio of ceramide:S1P may constitute a physiological rheostat regulating in numerous cellular processes[5].

Here, we demonstrate that adiponectin exerts its beneficial metabolic effects through a lowering of cellular ceramide levels mediated by activation of its cognate receptors AdipoR1 and AdipoR2. Our data establishes a connection between the vast literature on adiponectin effects and the observations that link altered levels of ceramides and its metabolites with changes in insulin sensitivity, inflammation, and survival.

Results

Adiponectin lowers ceramide levels independent of AMPK

We examined relationships between adiponectin and sphingolipid metabolism in several models of insulin resistance. The *lep*$^{ob/ob}$ mouse with its characteristic hyperlipidemic profile that is associated with hypoadiponectinemia offers an ideal setting to study this phenomenon. Compared to lean littermates, *lep*$^{ob/ob}$ livers had elevated ceramide levels. The

administration of recombinant adiponectin effectively reduced hepatic ceramide content (Fig. 1a). Adiponectin universally decreased all ceramide and dihydroceramide species, showing no discrimination for the acyl chain length or saturation of ceramides (Supplementary Fig. 1a). When performing euglycemic clamp studies in *lep*$^{ob/ob}$ mice, adiponectin injections caused an increase in the glucose infusion rate within 30–40 minutes (Fig. 1b). The ceramide-lowering effects of adiponectin happened within the same time frame (Supplementary Fig. 1b). Consistent with our previous studies[6],[2],[7], hepatic insulin sensitivity (but not muscle insulin sensitivity) was improved as demonstrated by an adiponectin-mediated lowering of hepatic glucose output during the clamp (Supplementary Fig. 1c&d). These results could not be explained by differences between blood glucose levels or plasma insulin concentrations during the clamps (Supplementary Fig. 1e&f).

We also tested whether adiponectin can exert similar effects under a physiologically more relevant high fat diet (HFD) feeding regimen. HFD increased hepatic ceramide content; the acute administration of recombinant adiponectin normalized ceramide levels (Fig. 1c). Acute adiponectin treatment did not lower DAG levels in either obese model (Supplementary Fig. 2a&b). The ceramide-lowering effects in the liver were cell autonomous, as adiponectin decreased palmitate-induced ceramide accrual in cultured H4iie hepatocytes from 2.19 +/− 0.07 fold over FFA-free BSA with PBS to 1.33±0.09 fold over BSA with adiponectin ($p<0.05$, n=6 from 3 separate experiments), while DAG remained elevated (6.42±0.16 vs 6.19±0.26).

Mice overexpressing adiponectin remained insulin sensitive after HFD, whereas mice lacking adiponectin showed an enhanced degree of insulin resistance (Fig. 1d). The hepatic ceramide content in the various adiponectin models mirrored the systemic insulin resistance, with adiponectin overexpressing mice displaying the lowest hepatic ceramide content, while adiponectin null mice carry considerably higher levels of ceramide in their livers after HFD exposure (Fig. 1e).

We tested the role of AMPK on adiponectin-mediated ceramide depletion using mice that conditionally lack the upstream kinase responsible for AMPK activation, LKB1. Injection of adenovirally encoded cre recombinase eliminated LKB1 from liver and decreased AMPK phosphorylation, as compared to adenoviral GFP treated control mice (Fig. 1f). Injection of recombinant adiponectin did not alter AMPK-mediated phosphorylation of ACC in LKB1$^{fl/fl}$ or LKB$^{-/-}$ livers. Furthermore, LKB1 expression in cardiac or skeletal muscle was not affected under these conditions (Supplementary Fig. 2c). As previously reported, adiponectin triggered a lowering of glucose levels in wild type rodents[8]. Although LKB1$^{-/-}$ mice have elevated basal glucose levels, injection of adiponectin also was highly effective at lowering circulating glucose levels (Fig. 1g). While adiponectin can activate AMPK under some conditions, it can normalize glucose levels independently of the kinase. Quantification of sphingolipids indicated that adiponectin reduced ceramide and glucosylceramide levels in the livers of wild type and LKB1$^{-/-}$ mice, but did not affect GM3 ganglioside abundance (Fig. 1h). Altered gene expression levels of some key components of the ceramide synthesis pathway and increased adiponectin receptor expression likely contributed to an altered basal level of ceramide and slight differences in the effectiveness of adiponectin (Supplementary Fig. 2d).

Anti-apoptotic effects of adiponectin on cardiac myocytes

We have previously described a number of models where we can conditionally induce apoptosis in selected cell types[9–10]. These animals express a target cell-specific transgene that comprises a cassette encoding a fusion protein consisting of procaspase 8 and a mutated FKBP dimerization domain (referred to as "ATTAC" mice - *A*poptosis *T*hrough *T*argeted *A*ctivation of *C*aspase 8). Injection of the compound AP20187 results in a pro-apoptotic cascade identical to the endogenous caspase 8–mediated apoptosis[10] without the upstream activation of death receptors[9,11]. We have generated an updated version of these mice that express the transgene in a cardiomyocyte specific fashion[11] ("HEART-ATTAC" mice). Maximal activation of this transgene through high-dose administration of AP20187 results in widespread apoptosis in the heart and death within 4 hours of administration (*Wang and Scherer, manuscript in preparation*). We have performed detailed dose responses to AP20187 and have optimized the protocol such that we obtain a mean 50% survival rate after 18 to 20 hours post administration of AP20187 in wildtype animals expressing the transgene (Fig. 2a). We have bred this transgene into mice with variable levels of adiponectin. Transgenic mice overexpressing adiponectin have 2- to 3-fold higher levels of adiponectin compared to wildtype[2], whereas mice that are heterozygous for a genetic deletion of the adiponectin locus have a 60% reduction in circulating adiponectin levels[7]. We have also examined the response in mice that completely lack adiponectin. The mean survival rate of the mice was dependent on the relative levels of adiponectin in the context of the HEART-ATTAC transgene (Fig. 2a). Elevated levels of adiponectin convey anti-apoptotic activity to the hearts of these mice, whereas mice with reduced levels or a complete lack of adiponectin are much more prone to death at the same dose of AP20187. Adiponectin levels do not have an impact on the expression level of the transgenic cassette (data not shown). Ceramide levels and adiponectin levels were generally inversely related: elevating adiponectin levels lowered both left ventricular as well as plasma ceramide concentrations (Fig. 2b). Furthermore, adiponectin null mice had significantly increased circulating levels of sphingomyelin compared to WT mice (2156±164 nmol/ml in nulls vs. 1413±150 nmol/ml in WT) ($n=6$ $p<0.01$), whereas a trend was apparent in adiponectin heterozygous mice that did not reach statistical significance. AP20187 did not induce cardiac ceramide accumulation (Supplementary Fig. 3a). Reduction of adiponectin was associated with a substantial decrease in S1P, dhS1P, dhSph and Sph (Fig. 2c). To investigate ceramides more directly as mediators of enhanced apoptotic susceptibility in the HEART-ATTAC mice, we pre-treated the animals with myriocin, an inhibitor of serine palmitoyl-CoA transferase (SPT), the key enzyme for ceramide biosynthesis. Myriocin caused a prolonged survival rate of the HEART-ATTAC mice due to a decrease in the concentration of ceramide. Moreover, direct administration of the S1P mimetic FTY720 triggered an improved survival rate that almost equaled the survival rate of adiponectin overexpressing HEART-ATTAC mice. Most notably, treating HEART-ATTAC mice with S1P (1mg/kg, IP) just prior to AP20187 treatment prevented death in 100% of the animals tested (Fig. 2d). In order to determine whether this is a direct effect on cardiac myocytes or whether this may be due to systemic changes in these mice, we performed a series of *in vitro* experiments on primary neonatal ventricular cardiac myocytes from HEART-ATTAC transgenic mice. These cells were pre-treated with either vehicle (BSA), BSA supplemented with C2-ceramide, or BSA pre-conjugated with palmitate to enhance endogenous ceramide

synthesis. Palmitate was also added in combination with myriocin to screen for ceramide-independent effects of the fatty acid. While palmitate was sufficient to induce a low dose of apoptosis in these cells, the sub-threshold dose of ceramide was insufficient to promote apoptosis in the absence of AP20187. The cardiomyocytes were examined for cell survival after exposure to AP20187 or DMSO control (Fig. 2e). While ceramide and palmitate (but not palmitate with myriocin) exacerbated AP20187-induced apoptosis, treatment with adiponectin or S1P potently enhanced cardiac myocyte survival. Though we do not observe elevated S1P levels in the cardiac muscle of adiponectin transgenic mice, we do detect a 21% increase in circulating S1P compared to wildtype mice (Supplementary Fig. 3b). This is consistent with previous observations that S1P is secreted into the extracellular milieu, where it acts through a family of cognate G-protein coupled receptors. As chronic exposure of hearts to exogenous S1P has been associated with increased heart growth[12], we evaluated cardiac weights in multiple cohorts. Compared to WT littermates, cardiac hypertrophy was evident in 20 and 30 week-old adiponectin transgenic mice, while no significant differences were observed in 10-week old mice (Supplementary Fig. 3c).

Anti-apoptotic effects of adiponectin on pancreatic β cells

We noticed a highly specific accumulation of adiponectin in β cells when recombinant adiponectin was injected into adiponectin null mice (Fig. 3a). While subsequent immunohistological staining of the pancreas for insulin and adiponectin resulted in no detectable adiponectin signal in the adiponectin null mice as expected, the recombinant adiponectin accumulated with a high degree of specificity in pancreatic cells containing insulin with no detectable signal outside the endocrine pancreas.

To further define the effects of adiponectin on β cells, we took advantage of a mouse model of inducible β cell death, the PANIC-ATTAC mouse[9]. This mouse works under the same principles as the HEART-ATTAC mouse, but it expresses the transgene under the rat insulin promoter. Activation of the transgene results in β cell loss and concomitant hyperglycemia. We chose a low concentration of AP20187 that triggers only modest hyperglycemia in PANIC-ATTAC mice on a wildtype background. In contrast, under the same conditions, mice that overexpress adiponectin remained completely euglycemic (Fig. 3b) and retained significantly more pancreatic insulin content relative to wildtype mice (Fig. 3c). Histological analysis indicated that islet area remained significantly larger as adiponectin overexpressers were partially refractory to AP20187-induced islet loss (Fig. 3f & Supplementary Fig. 4a). While changes in adiponectin expression had no significant effects on islet size or insulin content in the absence of the PANIC-ATTAC transgene, the combination of ATTAC expression and adiponectin ablation resulted in substantially smaller islets (Fig. 3f & Supplementary Fig. 4a) and lower pancreatic insulin content (Supplementary Fig. 4b) in male mice, even in the absence of AP20187. Hyperglycemia emerged shortly after birth and became progressively higher up to 3 weeks of age (Supplementary Fig. 4c). The relevance of adiponectin for normal β cell function was further highlighted by impaired insulin secretion in response to arginine (Supplementary Fig. 4d) or glucose (Supplementary Fig. 4f), which contributed to much higher glucose excursions during glucose tolerance tests (Supplementary Fig. 4e). Female wild type PANIC-ATTAC mice (that have higher circulating adiponectin levels than their male counterparts) were more resistant to apoptosis.

However, adiponectin ablation enabled AP20187-induced hyperglycemia after aggressive dosing regimens (Fig. 3d). AP20187 administration resulted in enhanced loss of pancreatic insulin content (Fig 3e) and led to smaller islets (Supplementary Fig. 4g) in adiponectin null mice, suggesting an increased susceptibility to apoptosis.

To test whether these effects of adiponectin on pancreatic β cells are cell autonomous or indirect, we examined the anti-apoptotic potential of adiponectin *in vitro* on the INS-1 pancreatic β cell line. Addition of adiponectin lowered the frequency of palmitate- or ceramide-induced cell death (Fig. 4a). Moreover, adiponectin prevented palmitate-induced ceramide accumulation (Supplementary Fig. 5a). The inclusion of a sphingosine kinase inhibitor abolished the adiponectin-mediated increases in survival rates of these cells (Fig. 4b), suggesting that adiponectin-mediated cytoprotective effects critically depend on the generation of S1P. To evaluate the role of AMPK in the antiapoptotic action of adiponectin, we overexpressed a dominant negative (K45R) mutant of AMPK (dnAMPK) or wildtype AMPK by adenoviral delivery as previously described[13]. Impaired AICAR-stimulated phosphorylation of acetyl CoA carboxylase confirmed effective lowering of AMPK activity (not shown). While the dnAMPK exacerbated palmitate-induced ceramide accrual and enhanced palmitate-induced apoptosis, adiponectin still lowered ceramide levels (Supplementary Fig. 5a) and offered significant protection against palmitate or ceramide induced apoptosis (Supplementary Fig. 5b).

To examine the kinetics of ceramide metabolism in greater detail, we performed a time course of ceramide degradation upon addition of short chain ceramide to INS-1 cells in the presence or absence of adiponectin. Co-administration of adiponectin markedly reduced (endogenous) long-chain ceramide levels (Supplementary Fig. 5c) and led to a rapid and sustained lowering of ceramides within 20 minutes and effectively neutralized the externally added short-chain ceramide (Supplementary Fig. 5d). Sphingolipidomic analysis revealed that adiponectin up-regulated sphingosine, S1P, and dihydrosphingosine-1-phosphate, consistent with a model in which adiponectin deacylates ceramide or dihydroceramide via the activation of ceramidase enzymatic activity (Supplementary Fig. 5e).

We next chose to directly measure whether adiponectin alters cellular ceramidase activity. As the known ceramidase enzymes are classified by pH optima and homology[14], we conducted these assays under a number of different pH conditions. Adiponectin potently stimulated ceramidase activity at neutral pH (pH 6.5 to 7) (Fig. 4c). The deacylation of ceramide at neutral pH is enhanced by adiponectin in a dose-dependent manner (Supplementary Fig. 5f). As discussed above, ceramide and its phosphorylated degradation product S1P may form a “rheostat” that governs survival and proliferation[5]. To evaluate the effectiveness of S1P in INS-1 cells, we determined that the addition of S1P to ceramide or palmitate-treated cells prevented apoptosis of the cells (Fig. 4d, e).

Ceramidase activity is associated with adiponectin receptors

Expression cloning efforts resulted in the identification of two receptors, AdipoR1 and AdipoR2, which bind adiponectin[1]. The lack of these receptors causes systemic metabolic dysfunction. Mice lacking both receptors display a more pronounced metabolic dysfunction

than either individual receptor knockout[15]. The detailed downstream signaling events triggered by the activation of these receptors remain to be elucidated.

AdipoR1 and AdipoR2 belong to the PAQ Receptor family. Some PAQR family members enhance ceramidase activity[16]. 293-T cells were used as host cells for our experiments, a cell line that expresses the adiponectin receptors endogenously. Transfection of cDNAs encoding AdipoR1 or AdipoR2 significantly enhanced ceramidase activity compared to control transfections with vector alone, and this activity could be stimulated by the *in vitro* addition of adiponectin (Fig. 5a). Similar effects were obtained via co-transfection with adiponectin (data not shown). We took advantage of a series of conserved histidine residues that are preserved across many different ceramidases, including AdipoR1 and AdipoR2[16]. We mutated these critical histidine residues to arginines. Receptors carrying these mutations have decreased ceramidase activity (Fig. 5a), although these mutations did not affect the stability of either AdipoR1 or AdipoR2 expression by western blot (Fig. 5b). To better define the role of these receptors in the ceramide degradation pathway *in vivo*, we used adenoviral preparations that lead to an overexpression of AdipoR1 and AdipoR2 in the liver. Infection with these adenoviruses carrying the AdipoR1 and AdipoR2 open reading frames lead to a 2-fold elevation of receptor expression in the liver (not shown) and caused a significant increase in hepatic ceramidase activity (Fig. 5c). Infection with either receptor normalized of hepatic ceramide content after a lard-oil infusion (Fig. 5c). Similarly, hepatic overexpression of the receptors lead to an improvement in insulin sensitivity after HFD exposure (Fig. 5d) and a concomitant lowering of the HFD-induced elevation of hepatic ceramide content (Fig. 5e).

To further evaluate the role of adiponectin receptors as mediators of adiponectin's ceramide lowering effects *in vitro*, we generated Murine Embryonic Fibroblasts (MEFs) lacking both AdipoR1 and AdipoR2 (double knockout, “DKO”). Once in culture, these cells grew at a comparable rate to MEFs isolated from wildtype mice, had no obvious changes in morphology, nor possessed any other distinctive features from wildtype cells under normal growth conditions. Treatment of wildtype MEFs with adiponectin stimulated ceramidase activity. However, MEFs lacking both adiponectin receptor isoforms displayed impaired ceramidase activity, and adiponectin fails to enhance the activity (Fig. 6a). Consistent with the observation that adiponectin-receptor deficient fibroblasts had lower ceramidase activity, these cells also displayed diminished accrual of S1P and dihydroS1P (Fig. 6b). This altered accrual of phosphorylated sphingoid bases was evident under basal conditions and after stimulation with palmitate; however the sphingosine and dihydrosphingosine were unaltered. Culturing wildtype MEFs with palmitate compared with BSA alone led to a marked increase of ceramide levels. Treatment with recombinant adiponectin compared to vehicle resulted in a lowering of cellular ceramide levels as expected (Fig. 6c). Baseline ceramide levels were significantly increased in MEFs from DKO animals, and ceramide levels further escalated upon incubation with palmitate. In contrast to wildtype MEFs, the addition of adiponectin to these cells did not reduce ceramide levels (Fig. 6c). To test whether these adiponectin-induced effects on ceramide levels are mediated through AMPK, we performed the same experiment with MEFs isolated from LKB1 null mice. LKB1 is essential for adiponectin-induced AMPK activation[17]. Cells derived from these mice

displayed a profound loss of AMPK phosphorylation (Thr-172) and diminished signaling in response to typical activators of the kinase, such as AICAR[18]. In LKB1 deficient fibroblasts, exposure to palmitate enhanced ceramide accrual, whereas addition of adiponectin lowered ceramide concentrations to the same extent as in wildtype MEFs (Fig. 6c). The concomitant changes in ceramide and S1P levels resulting from deletion of both adiponectin receptors produced a 5 times greater ratio of ceramide:S1P than WT cells suggesting susceptibility to cell death. To explore these effects on cell survival, we incubated MEFs with palmitate and assayed viability. Wildtype MEFs died to a low but measureable extent under the conditions chosen, and addition of recombinant adiponectin reduced the incidence of cell death (Fig. 6d). MEFs from DKO mice were much more susceptible to lipid-induced cell death, and adiponectin could not improve cell survival rates (Fig. 6d). However, addition of S1P completely rescued these cells from cell death (Supplementary Fig. 6a). While MEFs isolated from LKB1 knockout mice are more susceptible to the lipotoxic effects of palmitate exposure, adiponectin increases the survival rate dramatically, consistent with its pro-survival actions being largely AMPK-independent. Furthermore, we have tested whether the adiponectin-related effects influence membrane ceramide levels in these cells. We have isolated membrane raft structures from wildtype MEFs and DKO MEFs that were either left untreated or treated with adiponectin. Membrane raft-associated ceramide content was significantly higher in the DKO MEFs and unaffected by adiponectin treatment; whereas it was lower in rafts derived from wildtype cells and further lowered by adiponectin (Supplementary Fig.6b).

Although these data collectively suggest that changes in ceramide and cell survival can occur independently of AMPK, they do not preclude the possibility that AMPK activation may occur downstream or independently of ceramidase activation. We directly assessed the phosphorylation of AMPK at serine 172 after the addition of adiponectin or sphingolipid in the presence or absence of the ceramidase inhibitor D-e-MAPP [1(S),2(R)-D-erythro-2-(N-myristoylamino)-1-phenyl-1-propanol]. In cultured INS-1 beta cells, full-length wildtype adiponectin, truncated globular adiponectin, S1P, and C2-ceramide all promoted AMPK phosphorylation (Fig. 6e). Ceramidase inhibition prevented AMPK phosphorylation as induced by both forms of adiponectin and C2-ceramide, but did not prevent AICAR or S1P from promoting phosphorylation. Identical results were seen in cultured C2C12 myotubes, where adiponectin's link to AMPK was first observed (data not shown). The activation of AMPK by C2-ceramide is perplexing, but is likely mediated by ceramide metabolism into sphingosine or S1P rather than ceramide itself. Consistent with that concept, ceramidase inhibition prevented the effect of ceramide on AMPK phosphorylation, and addition of a ceramide analog to INS-1 cells promoted an astounding 57-fold increase in S1P ($P<0.01$, $n=4$).

Discussion

The physiological actions of adiponectin are very diverse. Elevated levels of adiponectin are correlated with improved metabolic parameters. Chronic elevation of adiponectin through either the use of a transgene or pharmacologically through treatment with PPARγ agonists dramatically enhances metabolic health in mice. Phenotypic changes in adiponectin mouse models are more dramatic upon exposure to a high fat diet or when bred into the *lep*$^{ob/ob}$

background. Clinically, adiponectin levels are an excellent systemic parameter reflecting the overall health of adipose tissue.

Ceramide promotes a diverse array of activities related to metabolic disease, often in direct opposition to adiponectin[19]. Targeted disruption of ceramide or glucosylceramide accumulation improves insulin action and promotes β-cell survival, akin to the actions of adiponectin[20]–[23]. Recent work has identified ceramide as a critical factor for toll like receptor 4-mediated antagonism of insulin action (*Holland and Summers, under review*). The anti-inflammatory effects of adiponectin may therefore be directly associated with ceramide depletion.

In hepatocytes, cardiomyocytes and β-cells, our data uniformly suggest a role for adiponectin receptor-mediated ceramidase activity as a primary signaling mechanism by which the adipokine elicits its broad spectrum of effects (Fig. 6g). Recent reports have suggested that the “progesterone and adiponectin Q receptor (PAQR) family” of proteins share homology with alkaline ceramidase and, in yeast, and can convey ceramidase activity in cells lacking the only known ceramidase isoform[16]. In mammalian cells, it remains unclear if adiponectin receptors themselves possess ceramidase activity, or sequester and activate ceramidase upon activation. Our mutational analysis of critical residues within the receptors suggests, but does not prove, that the activity may be an integral component of the receptors themselves. Of note, the ceramidase activity associated with adiponectin displays less substrate specificity than previously studied ceramidase isoforms[24]. Collectively, these studies suggest that adiponectin receptors may serve a fundamental role in the physiological regulation of ceramide and S1P balance.

Recently, adiponectin and AdipoR1 were shown to induce extracellular calcium influx that leads to an increased PGC-1α activity and enhanced mitochondrial biogenesis[17]. While we question the role of AMPK as an upstream mediator of adiponectin's actions in liver, we want to emphasize that the results presented here are consistent with the downstream signaling model proposed by these authors[17]. We have previously shown that mice overexpressing adiponectin display a distinct upregulation of the entire mitochondrial program[2]–[3],[25]. Furthermore, they display a “browning” (i.e. enhanced brown adipocyte phenotype) of their white adipose tissue. Both of these are hallmarks of enhanced PGC1α activity in adipocytes and other tissues[26].

S1P has previously been demonstrated to activate AMPK[27] and ample evidence in the literature couples sphingosine and S1P with calcium influx, and release from the ER[28]–[29]. Our data confirm these relationships and suggest that ceramidase activity is an essential initiator of the broad spectrum of adiponectin actions. As such, the reported activation of AMPK observed in a subset of cell types may be a downstream event rather than an upstream activator of adiponectin action, mediated by a conversion of ceramides into S1P, which can also trigger an influx of calcium. The potential role of S1P in adiponectin-mediated AMPK activation suggests an explanation for the lack of adiponectin-induced AMPK activation in liver, despite effects on AMPK seen in extrahepatic tissues. S1P is secreted in HDL particles and is degraded in the liver[30], driven by high expression of its degrading enzyme sphingosine phosphate lyase, which is predominantly expressed in this

tissue[31]. In fact, hepatic S1P levels were below the limits for detection by mass spectrometry in our assays. In addition, work in other organisms[16],[32] suggests that the pathway from PAQR to AMPK may be through other kinases with homologs in humans, notably PKA and PDK, both of which may be stimulated by sphingoid bases and both of which play important roles in energy homeostasis. Thus, the insulin sensitizing effects of adiponectin on its primary target tissue, the liver, may be primarily influenced by ceramide catabolism rather than S1P accumulation.

Based on these findings, we would like to suggest a revised view of adiponectin signaling that has sphingolipid metabolism at its core (Fig. 6G).

Research Design and Methods

Animals

Mice were maintained on a 12 hr dark/light cycle and fed a normal chow diet. Unless otherwise indicated, all animals were 8–10 weeks old at the time of experiments. Animals were bred in house in the UTSW Medical Center and the Albert Einstein College of Medicine animal facilities. The high fat diet consisted of 60 E% from fat (Research Diets, D12492). The Institutional Animal Care and Use Committee of the University of Texas Southwestern Medical Center and the Albert Einstein College of Medicine approved all animal experimental protocols.

Generation and treatment of ATTAC animals and AdipoR1 and AdipoR2 null mice

HEART-ATTAC mice were generated as described for the previously described PANIC-ATTAC mice[9], except the transgene was driven by the myosin heavy chain promoter. This mouse is similar in design (except for the use of an updated FKBP cassette) as the mouse reported by Kitsis and colleagues[11]. The dimerizer AP20187 was administered according to the manufacturer recommendations[33] (Ariad Pharmaceuticals). AdipoR1- and AdipoR2-deficient mice were generated by Deltagen, Inc..

Materials

Full-length wildtype, and Cys39 murine adiponectin were produced from 293 cells as previously described[34]–[35]. Myriocin, fatty acid free BSA, palmitic acid, propidium iodide and Annexin VFITC were from Sigma. NBD stearate; NBD-C18, 16:0, 18:0, 20:0, 22:0, 24:0, 24:1 Ceramides; (Cer), 16:0, 18:0, 24:0, 24:1 Dihydroceramides (DHCer); 16:0, 18:0, 24:1 Glucosylceramides (GlcCer); 17:0 sphingosine-1-phosphate (S1P); C18:0 dihydroshpingosine-1-phosphate (SaS1P); and dihydrosphingosine (Sa) were from Avanti Lipids. C2-ceramide and diacylglycerol kinase were from EMD Biosciences. Blendzyme IV, BCA protein assay kits and TUNEL staining kits were obtained from Roche. AdipoR1, AdipoR2, and GFP adenoviruses were from Vector Biolabs.

Lipid quantification

Sphingolipid were quantified as described previously by LC/ESI/MS/MS using a TSQ Quantum Ultra-triple quadrupole mass spectrometer (Thermo Fisher) equipped with an

electrospray ionization (ESI) probe and interfaced with an Agilent 1100 HPLC (Agilent Technologies)[36]. Diacylglycerol was quantified as previously described[37].

Hyperinsulinemic-Euglycemic Clamps

Hyperinsulinemic clamps were performed on conscious, unrestrained, 10 week-old *lep*$^{ob/ob}$ mice (C57Bl6J) as previously described[38] using an Instech mouse infusion kit (Instech Labs) to allow free movement. An iv bolus of adiponectin (adn, 2mg/kg, IV, 120 minutes post insulin) or PBS (0.1mL) was given after achieving an initial clamped state.

Lipid infusions

Lard oil emulsions (20%) and glycerol emulsions were prepared as previously described[39]. Lipid-heparin emulsions were infused for 6 hours at previously established rates[40]. Conscious unrestrained mice were infused through jugular catheters as described for hyperinsulinemic clamps.

Tolerance Tests

Tolerance tests were performed as previously described[21]. Insulin tolerance tests were initiated with human insulin (0.75 mU/kg, IP) after a 3-hour fast. Glucose tolerance tests were initiated by injection of glucose (1 mg/g, IP) after a 6-hour fast. Arginine tolerance tests were initiated by injection of L-arginine (1mg/g, IP) after a 6-hour fast.

Ceramidase Activity Assays

The deacylation of C18-NBD-ceramide was determined from crude cell lysates using a slight modification of the previously described method[41]. Briefly, NBD-Ceramide (8nmol) was dried under inert gas and resuspended in 10 μL ceramide assay detergent to help solubilize the lipid (7.5% octyl-β-D-glucopyranoside, 5mM cardiolipin, 1 mM diethylenetriaminepenta-acetic acid, pH 7) and 10 μL of buffer A (25 mM BisTris (pH 6.5) 0.3% Nonidet P-40). To achieve different pH conditions, 25 mM BisTris (pH 6.5, pH7), 25 mM Ammonium Acetate (pH5), or 25 mM Tris (pH 7.5, pH 8.0, pH 9.5) were used to modify the pH of buffer A.

Immunoblot Analysis

Animal tissues were processed and western blots were developed as previously described[42]. Antibodies against LKB1, phosphorylated AMPK, AMPK were from Cell Signaling (Beverly, MA). Antibodies against phosphorylated ACC were from Upstate (Lake Placid, NY). Flag antibodies were from Sigma.

Isolation of neonatal cardiomyocytes

Primary neonatal ventricular cardiomyocytes were obtained from 1–5 day-old heart ATTAC transgenic pups as previously described methods[43].

Site-directed mutagenesis of AdipoR1 and AdipoR2

The cDNAs of both Adiponectin Receptors were amplified from mouse adipose tissue cDNA library by PCR. The cDNAs with the flag tag at 3' end were ligated into the BamH1

site (for R1) or into BamH1 and EcoR1 sites (for R2) of the pcDNA3.1 backbone. Site-directed mutagenesis of all constructs was carried out using the QuikChange kit according to the manufacturer's protocol (Stratagene). (Sequences of all PCR and mutagenesis primers are given in Supplemental Table I).

Cell Viability Assays

Following treatments, cells were analyzed by exclusion of trypan blue dye (0.4%). Solution was added 1:1 and allowed to stain for 3 minutes. Cells were immediately counted using a Cellometer (Nexcellom Biosciences). Analogous results were obtained by MTT Assays performed as previously described[44].

Microscopy and immunofluorescence

Exogenously administered adiponectin was visualized as previously described[45].

Flow Cytometry

Flow cytometry was carried out utilizing a Coulter EPICS V flow cytometer and Dako-Cytomation Cyclops software as previously described.[46]

Statistics

The results are shown as mean±SEM. All statistical analysis was performed in SigmaStat 2.03 (SysStat Software, Point Richmont, CA). Differences between multiple groups were determined by 2 way ANOVA. Tolerance tests were evaluated for significance based on summed area under the curve for each animal. Kaplan Meier plots were compared by log-rank test. For comparison between 2 independent groups the Students T-test were used. Significance was as accepted at $p < 0.05$.

Supplementary Material

Refer to Web version on PubMed Central for supplementary material.

Acknowledgements

We thank members of the Scherer and Summers laboratories for helpful comments. We would like to thank Dr. Richard Kitsis for helpful discussions regarding the generation of HEART-ATTAC mice. We thank Dr. Bob Hammer and the Transgenic Core Facility at UT Southwestern for the generation of the mouse models used in this study and the Metabolic Core Facility at UT Southwestern for help with phenotyping of the mice. LKB1$^{-/-}$ mice and cells were a kind gift from Ronald DePinho. INS-1 832/13 cells were generously provided by Chris Newgard. We thank Ariad Pharmaceuticals for providing the dimerization kit and compound AP20187. This work was supported by NIH grants R01-DK55758, R01-CA112023, RC1-DK086629 and P01-DK088761 (PES); R01-DK56886 or P01-DK49210 (MJB); as well as R21-DK073181 (SAS). WLH was supported by National Research Service Award (NRSA) F32-DK083866 and TL1-DK081181. JMR was supported by F32-DK085935 and T32-HL007360 and KED was supported by F32-DK081279. NH was funded by a grant from University of Copenhagen.

References

1. Yamauchi T, et al. Cloning of adiponectin receptors that mediate antidiabetic metabolic effects. Nature. 2003; 423:762–769. [PubMed: 12802337]
2. Combs TP, et al. A transgenic mouse with a deletion in the collagenous domain of adiponectin displays elevated circulating adiponectin and improved insulin sensitivity. Endocrinology. 2004; 145:367–383. [PubMed: 14576179]

3. Kim JY, et al. Obesity-associated improvements in metabolic profile through expansion of adipose tissue. J Clin Invest. 2007; 117:2621–2637. [PubMed: 17717599]
4. Holland WL, Summers SA. Sphingolipids, insulin resistance, and metabolic disease: new insights from in vivo manipulation of sphingolipid metabolism. Endocr Rev. 2008; 29:381–402. [PubMed: 18451260]
5. Takabe K, Paugh SW, Milstien S, Spiegel S. "Inside-out" signaling of sphingosine-1-phosphate: therapeutic targets. Pharmacol Rev. 2008; 60:181–195. [PubMed: 18552276]
6. Combs TP, Berg AH, Obici S, Scherer PE, Rossetti L. Endogenous glucose production is inhibited by the adipose-derived protein Acrp30. J Clin Invest. 2001; 108:1875–1881. [PubMed: 11748271]
7. Nawrocki AR, et al. Mice lacking adiponectin show decreased hepatic insulin sensitivity and reduced responsiveness to peroxisome proliferator-activated receptor gamma agonists. J Biol Chem. 2006; 281:2654–2660. [PubMed: 16326714]
8. Berg AH, Combs TP, Du X, Brownlee M, Scherer PE. The adipocyte-secreted protein Acrp30 enhances hepatic insulin action. Nat Med. 2001; 7:947–953. [PubMed: 11479628]
9. Wang ZV, et al. PANIC-ATTAC: a mouse model for inducible and reversible beta-cell ablation. Diabetes. 2008; 57:2137–2148. [PubMed: 18469203]
10. Pajvani UB, et al. Fat apoptosis through targeted activation of caspase 8: a new mouse model of inducible and reversible lipoatrophy. Nat Med. 2005; 11:797–803. [PubMed: 15965483]
11. Wencker D, et al. A mechanistic role for cardiac myocyte apoptosis in heart failure. J Clin Invest. 2003; 111:1497–1504. [PubMed: 12750399]
12. Brakch N, et al. Evidence for a role of sphingosine-1 phosphate in cardiovascular remodelling in Fabry disease. Eur Heart J. 2010; 31:67–76. [PubMed: 19773225]
13. Gleason CE, Lu D, Witters LA, Newgard CB, Birnbaum MJ. The role of AMPK and mTOR in nutrient sensing in pancreatic beta-cells. J Biol Chem. 2007; 282:10341–10351. [PubMed: 17287212]
14. Mao C, Obeid LM. Ceramidases: regulators of cellular responses mediated by ceramide, sphingosine, and sphingosine-1-phosphate. Biochim Biophys Acta. 2008; 1781:424–434. [PubMed: 18619555]
15. Yamauchi T, et al. Targeted disruption of AdipoR1 and AdipoR2 causes abrogation of adiponectin binding and metabolic actions. Nat Med. 2007; 13:332–339. [PubMed: 17268472]
16. Villa NY, et al. Sphingolipids function as downstream effectors of a fungal PAQR. Mol Pharmacol. 2009; 75:866–875. [PubMed: 19066337]
17. Iwabu M, et al. Adiponectin and AdipoR1 regulate PGC-1alpha and mitochondria by Ca(2+) and AMPK/SIRT1. Nature. 2010
18. Shaw RJ, et al. The tumor suppressor LKB1 kinase directly activates AMP-activated kinase and regulates apoptosis in response to energy stress. Proc Natl Acad Sci U S A. 2004; 101:3329–3335. [PubMed: 14985505]
19. Holland WL, Scherer PE. PAQRs: a counteracting force to ceramides? Mol Pharmacol. 2009; 75:740–743. [PubMed: 19158359]
20. Aerts JM, et al. Pharmacological Inhibition of Glucosylceramide Synthase Enhances Insulin Sensitivity. Diabetes. 2007
21. Holland WL, et al. Inhibition of ceramide synthesis ameliorates glucocorticoid-, saturated-fat-, and obesity-induced insulin resistance. Cell Metab. 2007; 5:167–179. [PubMed: 17339025]
22. Zhao H, et al. Inhibiting glycosphingolipid synthesis improves glycemic control and insulin sensitivity in animal models of type 2 diabetes. Diabetes. 2007; 56:1210–1218. [PubMed: 17470562]
23. Yamashita T, et al. Enhanced insulin sensitivity in mice lacking ganglioside GM3. Proc Natl Acad Sci U S A. 2003; 100:3445–3449. [PubMed: 12629211]
24. El Bawab S, et al. Substrate specificity of rat brain ceramidase. J Lipid Res. 2002; 43:141–148. [PubMed: 11792733]
25. Asterholm IW, Scherer PE. Enhanced metabolic flexibility associated with elevated adiponectin levels. Am J Pathol. 2010; 176:1364–1376. [PubMed: 20093494]

26. Puigserver P. Tissue-specific regulation of metabolic pathways through the transcriptional coactivator PGC1-alpha. Int J Obes (Lond). 2005; 29(Suppl 1):S5–9. [PubMed: 15711583]
27. Levine YC, Li GK, Michel T. Agonist-modulated regulation of AMP-activated protein kinase (AMPK) in endothelial cells. Evidence for an AMPK -> Rac1 -> Akt -> endothelial nitric-oxide synthase pathway. J Biol Chem. 2007; 282:20351–20364. [PubMed: 17519230]
28. Spiegel S, Milstien S. Sphingosine-1-phosphate: an enigmatic signalling lipid. Nat Rev Mol Cell Biol. 2003; 4:397–407. [PubMed: 12728273]
29. Olivera A, et al. The sphingosine kinase-sphingosine-1-phosphate axis is a determinant of mast cell function and anaphylaxis. Immunity. 2007; 26:287–297. [PubMed: 17346996]
30. Karliner JS. Sphingosine kinase and sphingosine 1-phosphate in cardioprotection. J Cardiovasc Pharmacol. 2009; 53:189–197. [PubMed: 19247197]
31. Van Veldhoven PP, Gijsbers S, Mannaerts GP, Vermeesch JR, Brys V. Human sphingosine-1-phosphate lyase: cDNA cloning, functional expression studies and mapping to chromosome 10q22(1). Biochim Biophys Acta. 2000; 1487:128–134. [PubMed: 11018465]
32. Kupchak BR, et al. Probing the mechanism of FET3 repression by Izh2p overexpression. Biochim Biophys Acta. 2007; 1773:1124–1132. [PubMed: 17553578]
33. Clackson T, et al. Redesigning an FKBP-ligand interface to generate chemical dimerizers with novel specificity. Proc Natl Acad Sci U S A. 1998; 95:10437–10442. [PubMed: 9724721]
34. Pajvani UB, et al. Structure-function studies of the adipocyte-secreted hormone Acrp30/adiponectin. Implications fpr metabolic regulation and bioactivity. J Biol Chem. 2003; 278:9073–9085. [PubMed: 12496257]
35. Schraw T, Wang ZV, Halberg N, Hawkins M, Scherer PE. Plasma adiponectin complexes have distinct biochemical characteristics. Endocrinology. 2008; 149:2270–2282. [PubMed: 18202126]
36. Li Z, et al. Liver-specific deficiency of serine palmitoyltransferase subunit 2 decreases plasma sphingomyelin and increases apolipoprotein E levels. J Biol Chem. 2009; 284:27010–27019. [PubMed: 19648608]
37. Perry DK, Bielawska A, Hannun YA. Quantitative determination of ceramide using diglyceride kinase. Methods Enzymol. 2000; 312:22–31. [PubMed: 11070860]
38. Berglund ED, et al. Fibroblast growth factor 21 controls glycemia via regulation of hepatic glucose flux and insulin sensitivity. Endocrinology. 2009; 150:4084–4093. [PubMed: 19470704]
39. Stein DT, et al. The insulinotropic potency of fatty acids is influenced profoundly by their chain length and degree of saturation. J Clin Invest. 1997; 100:398–403. [PubMed: 9218517]
40. Kim JK, et al. PKC-theta knockout mice are protected from fat-induced insulin resistance. J Clin Invest. 2004; 114:823–827. [PubMed: 15372106]
41. Mao C, et al. Cloning and characterization of a novel human alkaline ceramidase. A mammalian enzyme that hydrolyzes phytoceramide. J Biol Chem. 2001; 276:26577–26588. [PubMed: 11356846]
42. Mu J, Brozinick JT Jr. Valladares O, Bucan M, Birnbaum MJ. A role for AMP-activated protein kinase in contraction- and hypoxia-regulated glucose transport in skeletal muscle. Mol Cell. 2001; 7:1085–1094. [PubMed: 11389854]
43. Burger D, et al. Erythropoietin protects cardiomyocytes from apoptosis via up-regulation of endothelial nitric oxide synthase. Cardiovasc Res. 2006; 72:51–59. [PubMed: 16904088]
44. Hohmeier HE, Tran VV, Chen G, Gasa R, Newgard CB. Inflammatory mechanisms in diabetes: lessons from the beta-cell. Int J Obes Relat Metab Disord. 2003; 27(Suppl 3):S12–16. [PubMed: 14704737]
45. Halberg N, et al. Systemic fate of the adipocyte-derived factor adiponectin. Diabetes. 2009; 58:1961–1970. [PubMed: 19581422]
46. He L, Fox MH. Variation of heat shock protein 70 through the cell cycle in HL-60 cells and its relationship to apoptosis. Exp Cell Res. 1997; 232:64–71. [PubMed: 9141622]

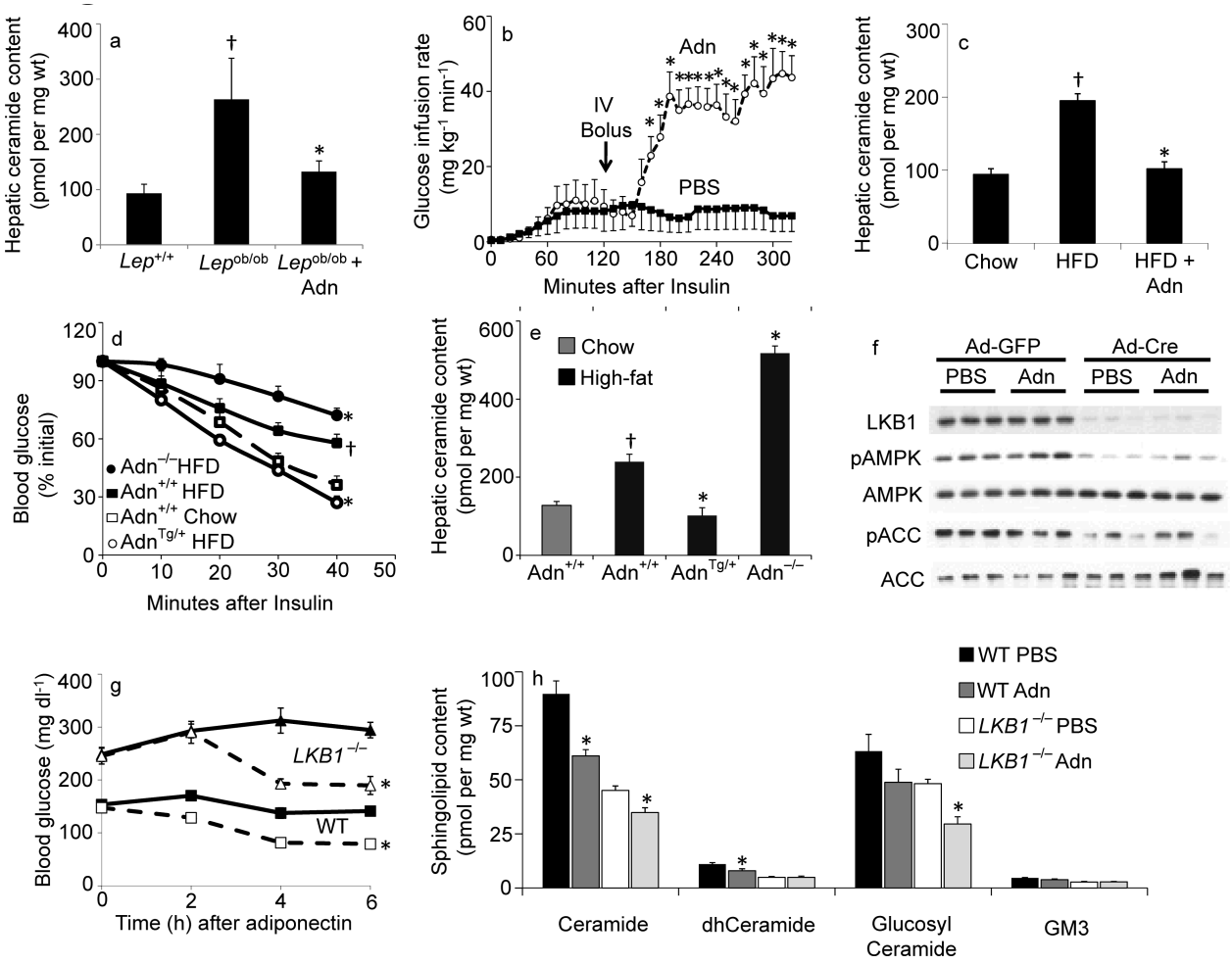

Fig 1. Adiponectin rapidly lowers hepatic ceramide content and improves glucose homeostasis

(**a**) Total ceramide levels were quantified from liver of leptin deficient (ob/ob) mice after 60-minute treatments with full length adiponectin (Adn, 2 mg/kg, IV) or PBS (n=6/group). (**b**) Glucose infusion rates were calculated during hyperinsulinemic-euglycemic clamps peformed on conscious unrestrained ob/ob mice before and after a bolus of adiponectin (Adn, 2 mg/kg, IV) or PBS (n=5/group). (**c**) Total ceramide levels were quantified from liver of diet induced obese mice after 60-minute treatments with full length adiponectin (Adn, 2 mg/kg, IV) or PBS (n=9/group). (**d–e**) Adiponectin deficient ($^{-/-}$), wildtype (+/+), or overexpressing mice (+/Tg) were maintained on high-fat diets (solid lines) or normal chow (dashed line) for 8 weeks prior to determination of (**d**) insulin tolerance and (**e**) hepatic ceramide content (n=7/group). (**f–h**) LKB1($^{fl/fl}$) mice were infected with adenovirus encoding either GFP or Cre recombinase 16 days prior to experiments (n=8/group). (**f**) Western blots of liver proteins probing against LKB1, phospho(T172)-AMPK, AMPK, phosphor(S79)-ACC1, and ACC1 (displayed in triplicate). (**g**) Whole blood glucose was monitored for 6 hours following injection of PBS (solid lines) or adiponectin (34 mg/kg, IV, dashed line). (**h**) Total hepatic sphingolipid levels were quantified by tandem MS/MS. * denotes significant effect of adiponectin ($p<0.01$). † Denotes significant effect of as compared to lean wildtype controls ($p<0.05$).

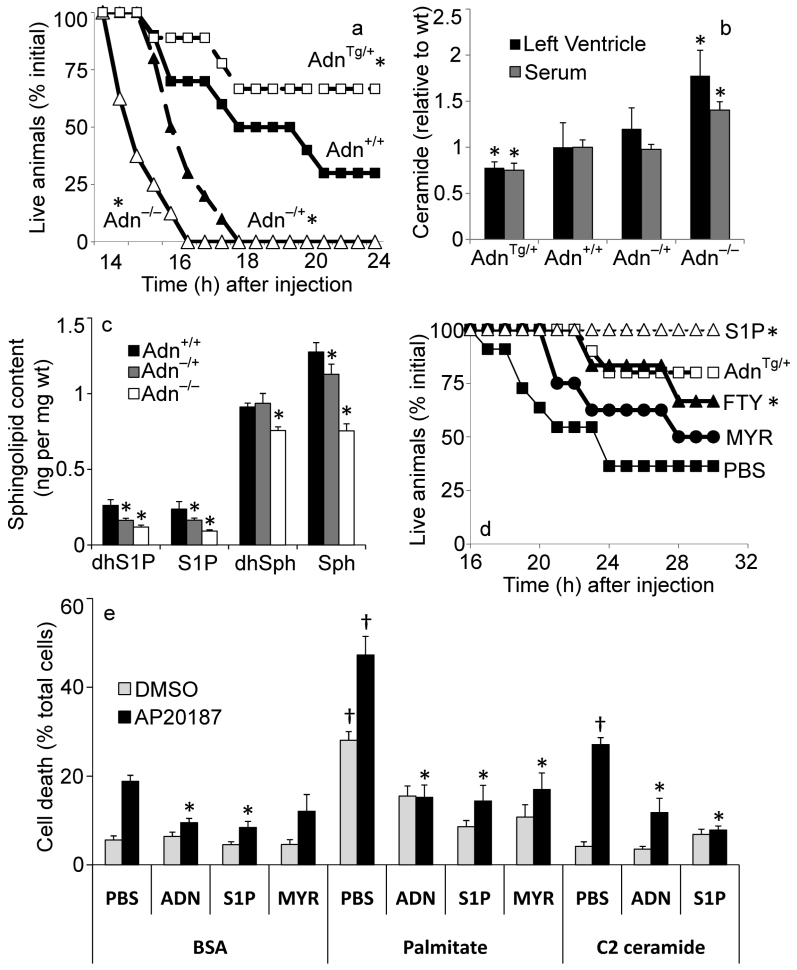

Fig 2. Adiponectin promotes cardiomyocyte and Heart ATTAC survival

(**a**) Female heart ATTAC transgenic mice crossed into indicated adiponectin backgrounds were challenged with AP20187 (0.010 μg/kg, IP) and survival was recorded as a Kaplan-Meier plot (n=12/group). (**b**) Ceramide was quantified from left ventricle or serum and normalized to the average content from adiponectin wildtype mice (63.9 pmol/mg in left ventricle, 9.5 pmol/μL in serum) (n=12/group). (**c**) Sphingosine, dihyrosphingosine, S1P, and dihydroS1P were quantified in left ventricle of WT (+/+), adiponectin (−/+), and adiponectin null mice (n=6/group). (**d**) Male HEART-ATTAC mice were treated with myriocin (0.3 mg/kg, IP), FTY720 (1 mg/kg, IP), S1P (1mg/kg, IP) or PBS immediately prior to injection with AP20187 (0.05 μg/kg, IP) and survival was recorded as a Kaplan-Meier plot (n=10/group). Additionally, treating HEART-ATTAC mice with S1P (1mg/kg, IP) just prior to AP20187 treatment prevented death in 100% of the animals tested (n=15) (**e**) Primary cardiomyocytes were isolated from heart ATTAC transgenic pups. After 72 hours of maintenance, cells were washed and treated with 2% BSA conjugated with: C2-ceramide (10 μM), myriocin (10 μM), palmitate (375 μM), or palmitate plus myriocin. PBS, adiponectin (3 μg/mL), or S1P (1 μM) were immediately added. Apoptosis was initiated by the addition of AP20187 (6.25 ng/mL), and viability was determined after 16 hours (n=6/

group from 3 separate experiments). * denotes significant ($p<0.05$) difference from WT control. † denotes significant ($p<0.01$) effect of lipid treatment.

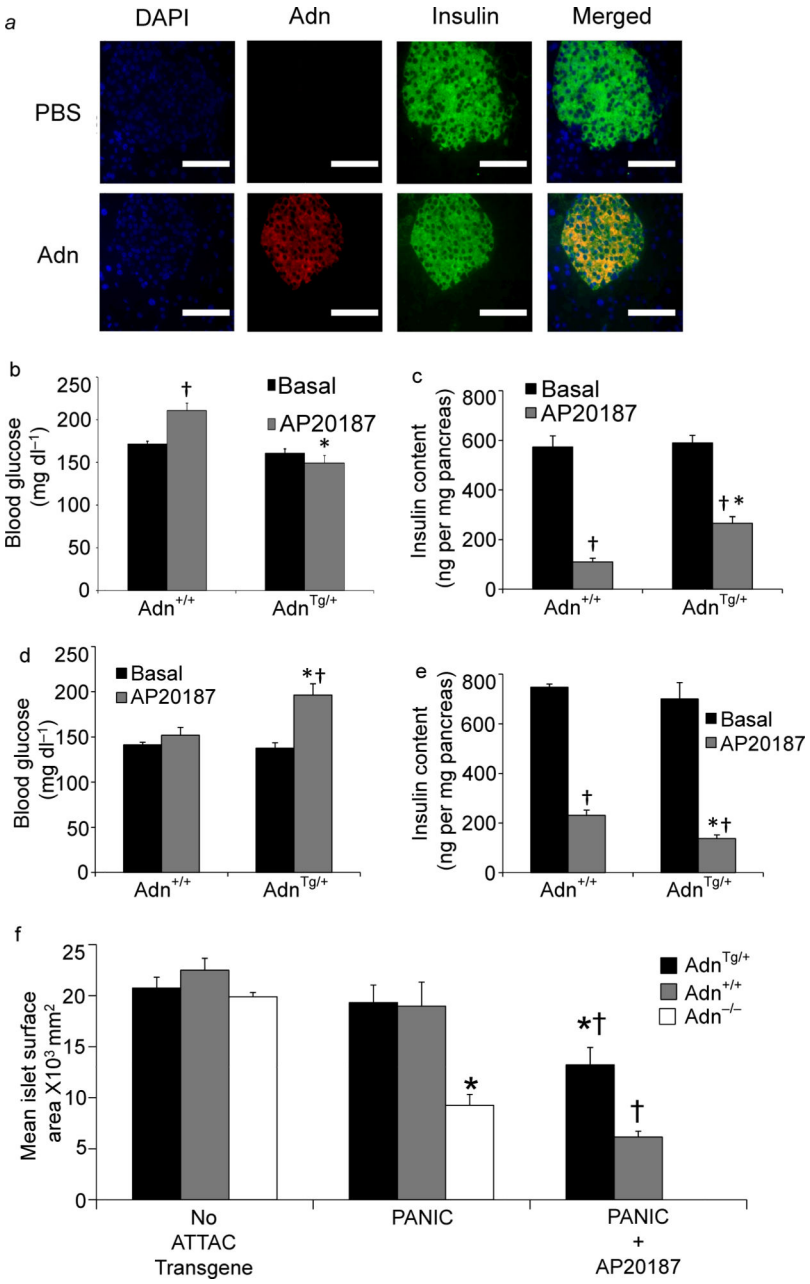

Fig 3. Adiponectin targets the endocrine pancreas and maintains β-cell mass

(**a**) Adiponectin, insulin, and nuclei were visualized by immunofluorescence after injection into adiponectin null mice (bar=100μm). (**b**) Random-fed blood glucose was assessed in male adiponectin transgenic vs. wildtype mice before and 10 days after treatment with AP20187 (0.2 mg/kg, IP, single injection) (n=12/group). (**c**) Total pancreatic insulin content was quantified from pancreas harvested 10 days after AP20187 treatment (n=6/group). (**d–e**) Female adiponectin null and wildtype PANIC-ATTAC mice were evaluated 10 days after initiating treatment with AP20187 (0.2 mg/kg, IP, twice daily for 3 days) or vehicle. (**d**) Random fed blood glucose was determined by glucometer (n=12/group). (**e**) Total pancreatic insulin content was quantified (n=6/group). (**f**) Pancreata were obtained 10 days

after treatment with AP20187 (0.2 mg/kg) or vehicle from 10–12 week-old male mice overexpressing adiponectin (Tg/+), wildtype for adiponctin (+/+), or lacking adiponectin ($^{-/-}$). Islet size was calculated by mean cross-sectional area of multicelled islets and reported as microns^2/islet (n=6/condition). * denotes significant ($p<0.02$) difference between adiponectin transgenic (or adiponectin null) from WT animal of the same treatment. † denotes significant ($p<0.02$) effect of AP20187 treatment.

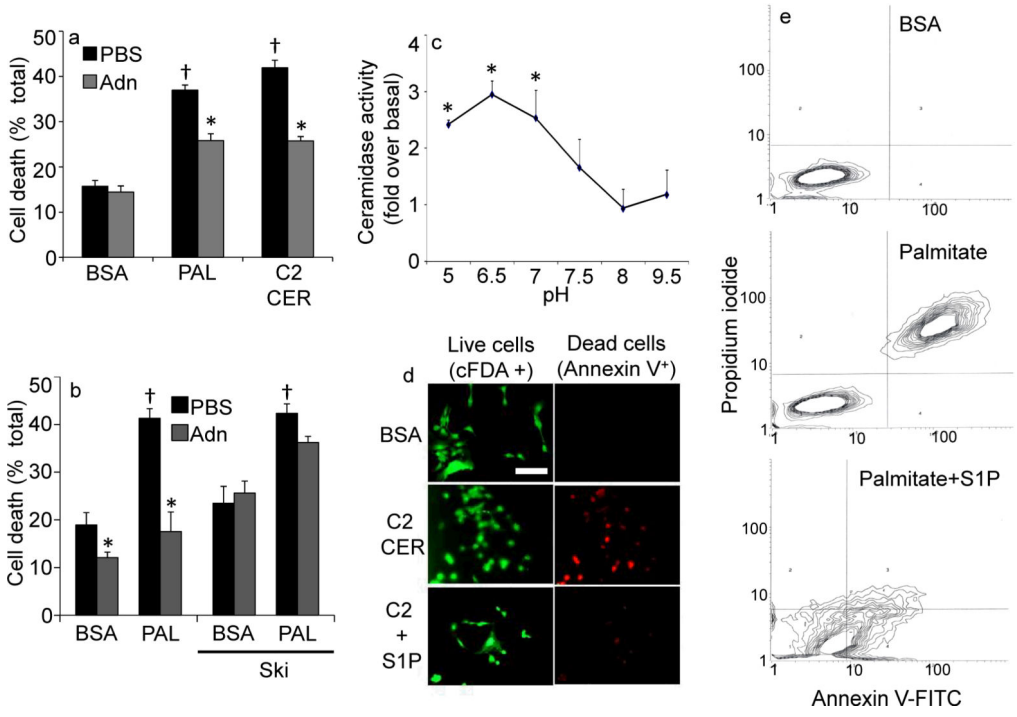

Fig 4. Adiponectin alters sensitivity to ceramide-induced apoptosis in INS-1 β-cells

(**a**) INS-1 cells were washed and removed to 2% BSA, Palmitate (750 μM in 2% BSA), or C2-Ceramide (50 μM in 2% BSA). Adiponectin (3 μg/mL) or PBS was immediately added and cell viability was determined after 18 hours (n=6/group from 3 separate experiments). (**b**) Cell viability was determined on INS-1 cells pretreated with sphingosine kinase inhibitor (2-(*p*-Hydroxyanilino)-4-(*p*-chlorophenyl) thiazole, 0.5 μM) or DMSO prior to delivery of adiponectin (3μg/mL) or PBS and maintained for 18 hours in the presence of 2% BSA or Palmitate (750 μM in 2% BSA) (**c**) Ceramidase activity was determined in lysates from cultured INS-1 cells under a range of pH conditions (n=4 from separate experiments) in the presence or absence of adiponectin (0.3 μg/mL, *in vitro*). "Fold change over baseline" refers to the change compared to BSA treatment without adiponectin. (**d**) INS-1 cells were challenged with C2-ceramide (50 μM) in the presence or absence of S1P (5 μM) cell death was determined by live/dead staining with cFDA or annexin V (image is representative of 3 separate experiments, bar=50μm). (**e**) Apoptosis of INS-1 cells was determined by FACS analysis of annexin V and propidium iodide stained cells following 18 hours of treatment with BSA, palmitate (750 μM), or coadministered palmitate and S1P (5μM) (representative of 3 independent experiments). * denotes significant ($p<0.01$) effect of adiponectin. † denotes significant ($p<0.01$) effect of pro-apoptotic insult.

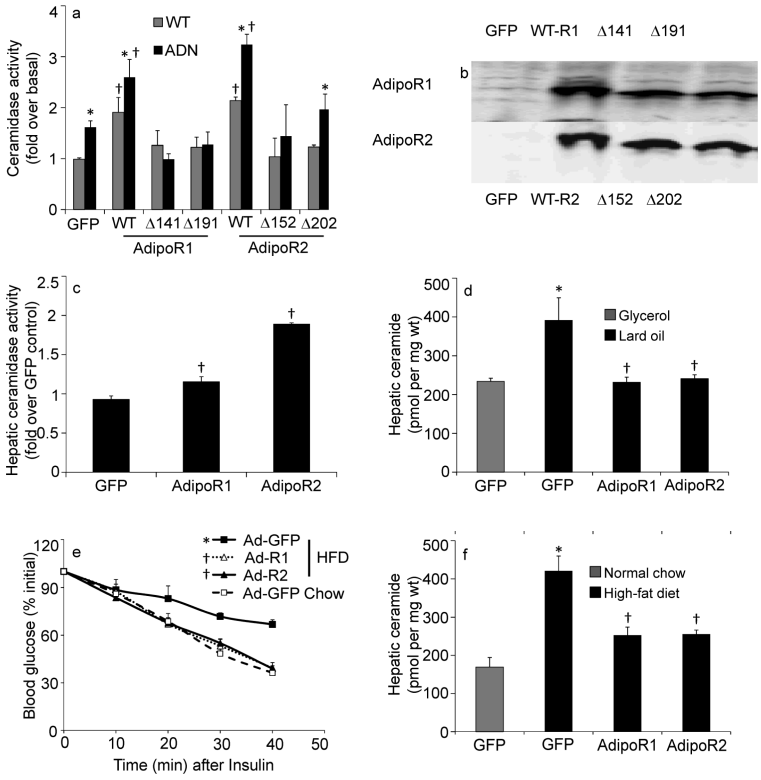

Fig 5. Adiponectin Receptors 1 and 2 convey ceramidase activity *in vivo*

(**a–b**) HEK-293T cells were transiently cotransfected with GFP and murine AdipoR1, murine AdipoR2, GFP alone, or indicated point mutants for conserved histidine residues in AdipoR1 (H141R or H191R) or AdipoR2 (H152R or H202R). Ceramidase activity after *in vitro* treatment with adiponectin (0.3 μg/mL) (**a**) and protein expression (**b**) were assessed 48 hours after transfection (n=5 from separate experiments). (**c–f**) Hepatic overexpression of human AdipoR1, human AdipoR2, or GFP was accomplished by adenoviral delivery (0.5 $\times 10^8$ PFU/mouse). (**c**) Hepatic ceramidase activity was determined from fresh lysates 5 days after infection of 9 week-old wildtype mice C57/Bl6J mice (n=5/group). (**d**) Hepatic ceramides were measured following 6 hour infusion of 20% lard oil emulsions or fat-free glycerol control emulsions (n=6/group). (**e–f**) After 8 weeks of maintenance on high-fat diets, wildtype FVB mice were infected with AdipoR1, AdipoR2, or GFP. Insulin tolerance (**e**) and hepatic ceramide content (**f**) were determined 8 days after infection (n=6–8/group). *denotes significant ($p<0.05$) effect of adiponectin or lipid administration. † denotes significant ($p<0.02$) effect of genetic overexpression.

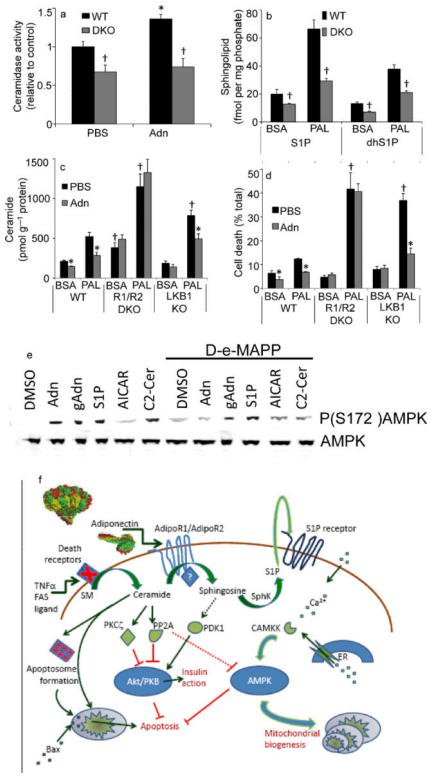

Fig 6. Ablating Adiponectin Receptors 1 and 2 impairs ceramidase activity, S1P generation and cell survival

(**a**) Ceramidase activity was determined from WT or AdipoR1/AdipoR2 double knockout (DKO) MEFs in the presence or absence of adiponectin (0.3 μg/mL, *in vitro*) (n=4). (**b**) S1P, and dihydroS1P were quantified from WT, or AdipoR1/AdipoR2 DKO MEFs after 12-hour incubation in palmitate (750 μM in 2% BSA) or BSA (2%) (n=6). (**c**) Ceramide levels were quantified from WT, AdipoR1/AdipoR2 DKO, or LKB1 knockout MEFs after 12-hour incubations with palmitate (750 μM in 2% BSA) or BSA (2%) supplemented with adiponectin (5 μg/mL) or PBS (n=6 from 3 separate experiments). (**d**) Cell viability was assessed in MEFs treated as in Fig. 6C after 16 hours of palmitate treatment. (n=5). (**e**) 60 minutes after removal from serum, cultured INS-1 cells were pretreated for 5 minutes with D-e-MAPP (100nM) or DMSO then treated for 10 minutes with full length adiponectin (Adn, 3μg/mL), truncated globular adiponectin (gAdn, 1 μg/mL), S1P (5 μM), AICAR (1 mM), or C2-ceramide (50 μM). Total and phosphorylated AMPK were probed by western blot (representative of 4 independent experiments). (**f**) Ceramide promotes apoptosis by aiding death receptor clustering, apoptosome formation, and Bax translocation. Ceramide impairs Akt activation via activation of PKCζ or PP2A. Adiponectin promotes the deacylation of ceramide by activating adiponectin receptors. The resulting sphingosine and S1P increase intracellular calcium and activate AMPK via stimulation of CAMKK. These actions promote survival, nutrient uptake, nutrient utilization and mitochondrial proliferation. * denotes significant ($p<0.05$) effect of adiponectin. † denotes $p<0.05$ compared to WT cells.